VOL. 19, NO. 15, AUGUST 2024 ISSN 1819-6608
ARPN Journal of Engineering and Applied Sciences

www.arpnjournals.com

A SPLIT RING RESONATOR SLOT BASED FABRICATED CRESCENT MICROSTRIP PATCH ANTENNAS FOR UWB WIRELESS SYSTEM APPLICATIONS

Haritha Thotakura[1], Merugumalli Rama Krishna[2], Nandamuri Siva Govind[3], P. Sanjay Krishnamal[3], G. Roopa Krishna Chandra[2], G. Vijaya Kumar[2] and K. Srinivasa Rao[2]
[1]Department of Electronics and Communication Engineering, PVP Siddhartha Institute of Technology, Vijayawada, India
[2]Department of Electronics and Communication Engineering, Andhra Loyola Institute of Engineering and Technology, Vijayawada, India
[3]Department of Electronics and Communication Engineering, PSCMR College of Engineering and Technology, Vijayawada, India
E-Mail: harithat4770@gmail.com

ABSTRACT

This paper clarifies significant bandwidth and optimum gain for a split ring resonator slot based fabricated microstrip patch antenna for ultra wide band (UWB) wireless telecommunication system applications. The antenna has a circular slot partially cut into a circular patch and radiates in the UWB frequency range. The design system features a steady radiation pattern and an impedance bandwidth of 3.3 to 10.96 GHz. The proposed UWB notch antenna is at 4.6 GHz, 7.29 GHz, and 9.36 GHz, with an impedance bandwidth of 3.3 to 10.96 GHz. The UWB notch antenna offers linear phase response and a group delay of fewer than 1 ns. It is practical for UWB applications due to less group delay and stable radiation patterns. FR4 material with a 4.4 relative permittivity. The reported antenna is measured following the manufacturing of the prototype design using HFSS simulations. The suggested fabricated antenna minimizes return loss. The findings demonstrate that when combined with VSWR 2, the reflection coefficient covers the band ranges from 3.3-10.96 GHz.

Keywords: UWB, s11, current distributions, radiation patterns.

Manuscript Received 15 June 2024; Revised 17 August 2024; Published 31 October 2024

1. INTRODUCTION

Microstrip antennas offer a wide range of uses in wireless communications because of their cost-effectiveness, portability, flexibility in design, and ease of production. Compact systems with multifunctionality are sought due to the rapid advancement of communication technology. The problem is to build multi-band antennas that do not require several antennas for various operating frequencies because antennas are an essential part of wireless systems and take up a lot of space. According to the literature, there are several multi-band configurations, each of which has a unique resonance frequency. These configurations include stacked patches, integrated patch antenna topologies, and combinations of metallic strips. Other standard structures incorporate various slots in the patch radiator, ground, and fractal geometry, which creates many resonant routes. This modern era of communication devices demands antennas that provide distinctive radiation characteristics with compact size [1]. Microstrip antennas promote ease of fabrication process. However, they need a dimension of half the size of the guided wavelength. Such larger dimension antennas make them accountable for getting better than other antennas, which could not be the solution for miniaturization. However, a few smaller antennas are available but suffer from the drawbacks of high cross-polarization and lower bandwidth [2]. A specification for a device is that it must attain multi-band with good far-field characteristics. Multiband devices promote a variety of applications at a time, removing the necessity for the large number of antennas that need huge areas and directing to compactness. Numerous designs have been outlined which produce a single band or multi bands [3]. However, these days there is a necessity for multiple bands that can be used for different applications.

Moreover, metamaterials can be utilized to accomplish the top tasks. They are productive homogeneous electromagnetic structures with remarkable properties like propagation constant less than 0 for β and ε. When $\mu < 0$ can now be defined as a mu-negative metamaterial. One of the finest examples of metamaterial is the Split ring resonator [4]. Antagonistic properties of SRR can be utilized to design a metamaterial model. Some literature works have demonstrated dual resonant band design. In [5], a metamaterial design is obtained with double bands. In [6], significant work is presented on the composite right- and left-handed resonant method that relies on boundary conditions and resonators according to order modes. In [7], an excellent dual-band metamaterial design with three-unit cells depending on zeroth order is reported. The invention's novelty is that its flipped stub is responsible for reducing the optimized area. Additionally, when the stub size increases, the operating frequency switches to a lower level, and virtual ground resonates at higher frequencies. A rectangular partial ground plane is reported to achieve one additional band, and the characteristic of the antenna provides good gain, bandwidth, and efficiency when compared with other designs. Multi-service wireless communication has seen significant growth in usage recently. Multi-band antennas are used in these modern multi-service wireless

communication systems [8]. Due to its intrinsic qualities, including its tiny size, lightweight, low cost, ease of manufacture, and integration with other RF components, the multi-band microstrip patch antenna is a perfect choice for wireless communication [8-10]. The typical microstrip patch antenna operates in a narrow frequency band. Its single resonance makes it capable of transmitting and receiving electromagnetic radiation for a single wireless communication application. The main drawbacks of traditional microstrip antennae are their narrow bandwidth and poor strength suitable for various wireless applications. For creating several operational frequency bands, a variety of approaches have been documented in the literature, including the use of slots/slits of various forms [11-14], multilayer stacks [15-18], and the folding of major radiating patches [19]. The development of communication systems has increased the demand for low-cost, lightweight antennas [20-23]. These antennas are anticipated to function well across a wide frequency band. The development of microstrip antennas is the result of this. Due to their accessibility, accessibility reduced geometrical design and other characteristics, microstrip antennas have a wide range of uses in wireless communication [24-27]. Since it is utilized for transmitting and receiving electromagnetic radiation, the antenna is an essential communication system component. The majority of applications for microstrip antennas include radar, GPS, GNSS, WLAN, WiMAX, UWB, etc. [28-31]. A radiation-emitting device is etched on a dielectric substrate to form the geometry of a microstrip antenna. On the back, the ground plane is visible. This work presents an enhanced gain triple-band inset-fed circular patch antenna in the current study for UWB (3.1-10.5 GHz) applications. A parasitic strip, one split ring resonator slot, and a circular patch construct this antenna. The frequency at which the common patch antenna operates is 3.3.to 10.96GHz. The recommended antenna's center frequencies of 4.6 GHz, 7.29 GHz, and 9.36 GHz, are obtained by adding three circular patches onto the radiating edges of the antenna. In this study, we provide three smaller circular patches mounted on the split ring resonator for a miniaturized circular microstrip patch antenna for triple-band applications.

2. ANTENNA DESIGN

The main ways that a radiating patch influences an antenna's performance are by changing its patterns, patterns, and surface current fields. The antenna's variety typically improves the performance of the patch in size and shape. But our goal is to understand how to get the desired outcomes. A straightforward circular patch was first explored. Figure-1 depicts the proposed circular slotted ring antenna's iterative stages.

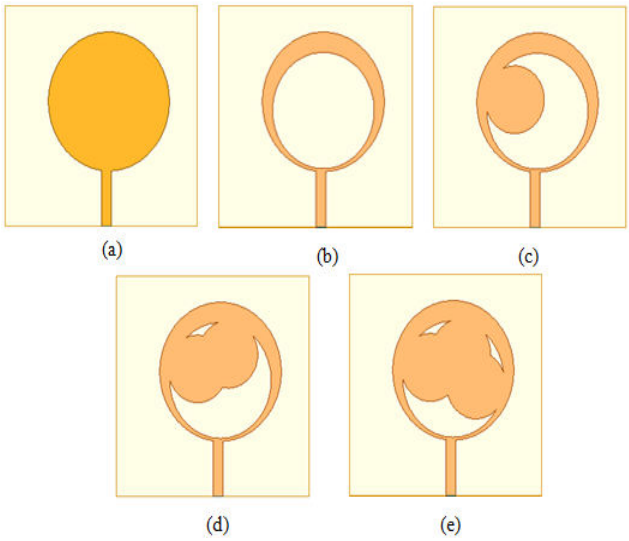

Figure-1. Steps to construct the crescent moon-shaped patch antenna.

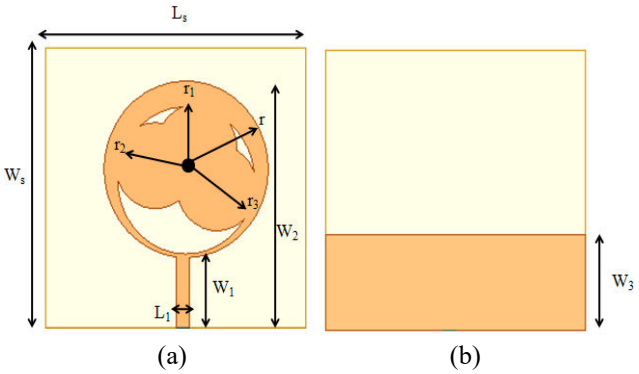

Figure-2. Geometry of the proposed antenna (a) top view (b) back view.

Table-1. Dimensions of the proposed crescent antenna.

Parameters	Dimension (mm)
L_s	38
W_s	38
L_1	2
W_1	12
W_2	34
W_3	13
r_1	5.8
r_2	5.8
r_3	5.8
r	12

The larger circular ring is then loaded with five circular annular rings. ANSYS HFSS, a program used to analyze mathematical equations based on engineering and mathematical expressions through finite element modelling, is used to simulate the antenna. The antenna's

geometry is shown in Figure-2. The suggested antenna's footprint measures 38 x 38 x 1.6 mm^3. The primary ring is initially loaded onto one inner circular ring. They are embedded together, two of them. The inner circular ring is then loaded with a set of three circular rings. The dimensions are optimized by analysis using the ANSYS program. The FR-4 substrate is used to manufacture the suggested antenna. The ground plane has dimensions of 38 x13 mm^2, while the inner radius of the giant circular ring is 8mm. Here, microstrip feeding is considered for the suggested design, and effective impedance matching is produced by selecting the ideal size. In Table-1, the parameters are listed.

3. RESULTS AND DISCUSSIONS

The circular patch antenna's optimum arrangement consists of three smaller circular rings encased in one another, as shown in Figure-2. The standard feed line was injected externally into the conducting patch. The simulations are carried out using the commercially available tool and the settings listed in Table-1. There are a total of five iterative phases recommended for this antenna. In Figure-1, the standard circular patch antenna represents the initial progression (a). A high reflection loss frequency was attained. It operates with impossible impedance. There are five steps in this iteration process. However, the desired frequency is achieved in the fifth iteration. Two circular patches of compact size are included in the larger outer ring in the fourth stage of Figure-1(d). In the final iteration, the frequency is achieved at the desired band, i.e., 10.96 GHz with a return loss of -33dB and -32 dB. Figure-3 illustrates the Iterative steps of the proposed geometry.

Figure-4 clarifies an analysis of the parameter W_1 in the proposed geometry. Figure-5 shows an analysis of the parameter W_3 in the proposed geometry. The created model is assessed using an analyzer, and the resulting figures are shown in Figure-6. Analysis of the parameter r in the proposed geometry is clarified in Figure-7.

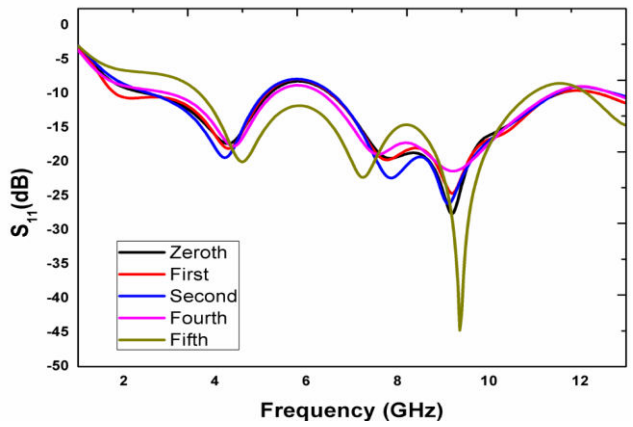

Figure-3. Iterative steps of proposed geometry.

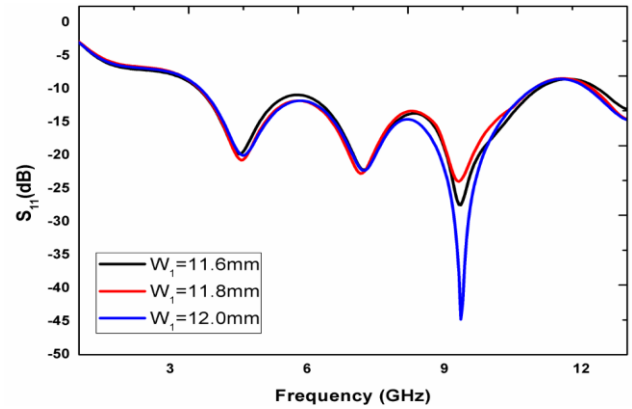

Figure-4. Analysis of the parameter W_1 in the proposed geometry.

Table-2. Values of the dual-band designed antenna.

Proposed antenna	Frequency (GHz)	Gain
Simulated	4.63 7.29 9.36	4.8 5.1 6.2
Measured	4.8 6.9 9.31	5.4 5.2 4.6

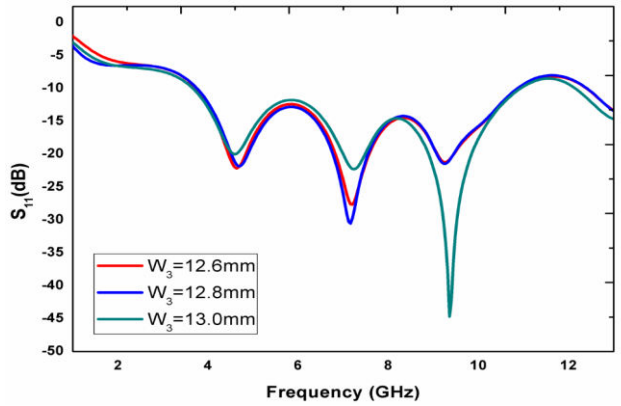

Figure-5. Analysis of the parameter W_3 in the proposed geometry.

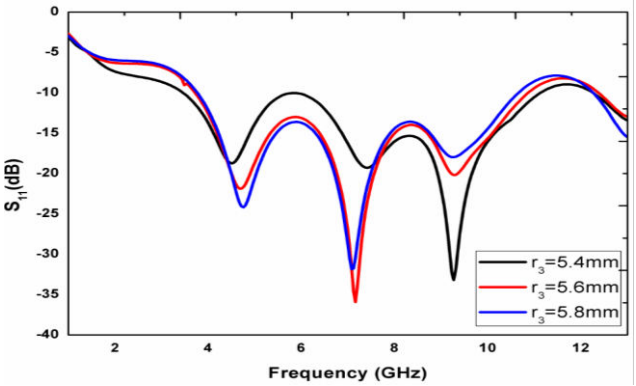

Figure-6. Analysis of the parameter r_3 in the proposed geometry.

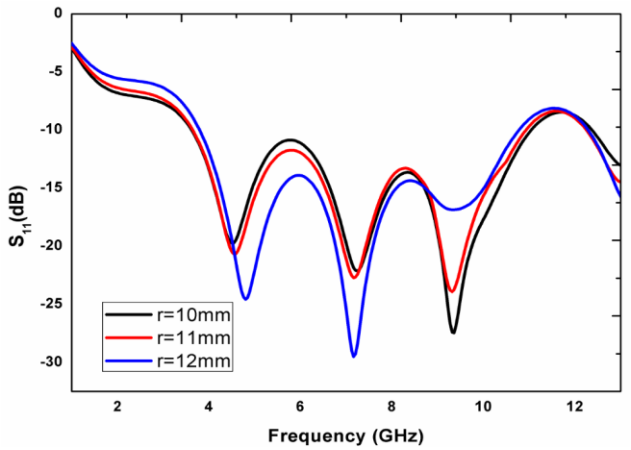

Figure-7. Analysis of the parameter r in the proposed geometry.

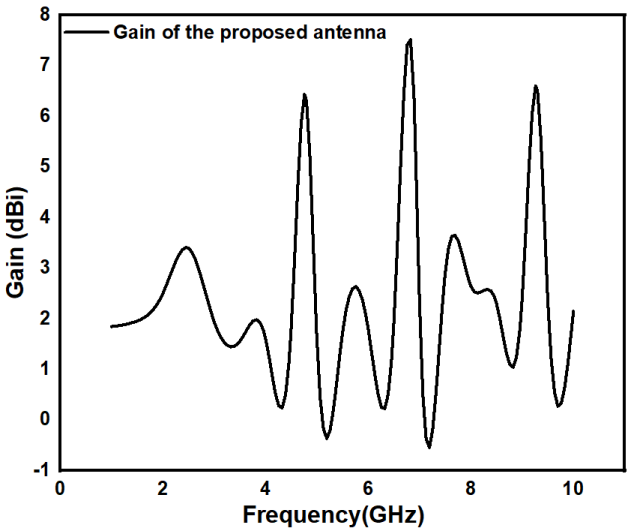

Figure-8. Gain the value of the suggested UWB antenna.

Figure-8 clarifies the analytical Gain of the suggested UWB antenna. The proposed antenna states the gain value of 6.51 across the operating frequency. An impedance of 50 ohms is achieved using the proposed device. The parametric study is also observed for the compact inner circular patch radius, and the distance is varied between the inner circular ring and the outer ring. The parameter W_1 is studied for different case studies. The length of the feed line is tuned to achieve the desired band and reflection loss in the final iterative step. When W_3= 2.5 mm, the design accomplishes a good return loss. The case studies of parameters like r and r_3 are displayed in Figure-6 and Figure-7. The obtained results of the device are tabulated in Table-2.

4. MODEL FABRICATION

Figure-9 shows the crescent patch antenna model that was created. The figure showed the simulated model, the fabricated model in the front view, and the fabricated model in the back picture with half the ground. The half ground is taken into consideration in this study to improve the antenna's properties. There is, nevertheless, a minimal difference between the simulated and measured values. Figure-10 compares the simulation and experimental data, showing that the variance is microscopic. The suggested device minimizes return loss. The crescent antenna is miniaturized and suitable for a variety of applications. In the picture below, photographs of the crescent antenna are also included.

Figure-9. Proposed antenna fabricated model.

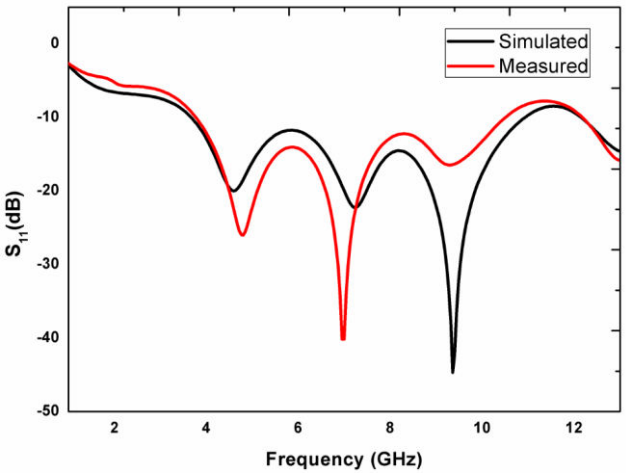

Figure-10. Measured results of the UWB antenna.

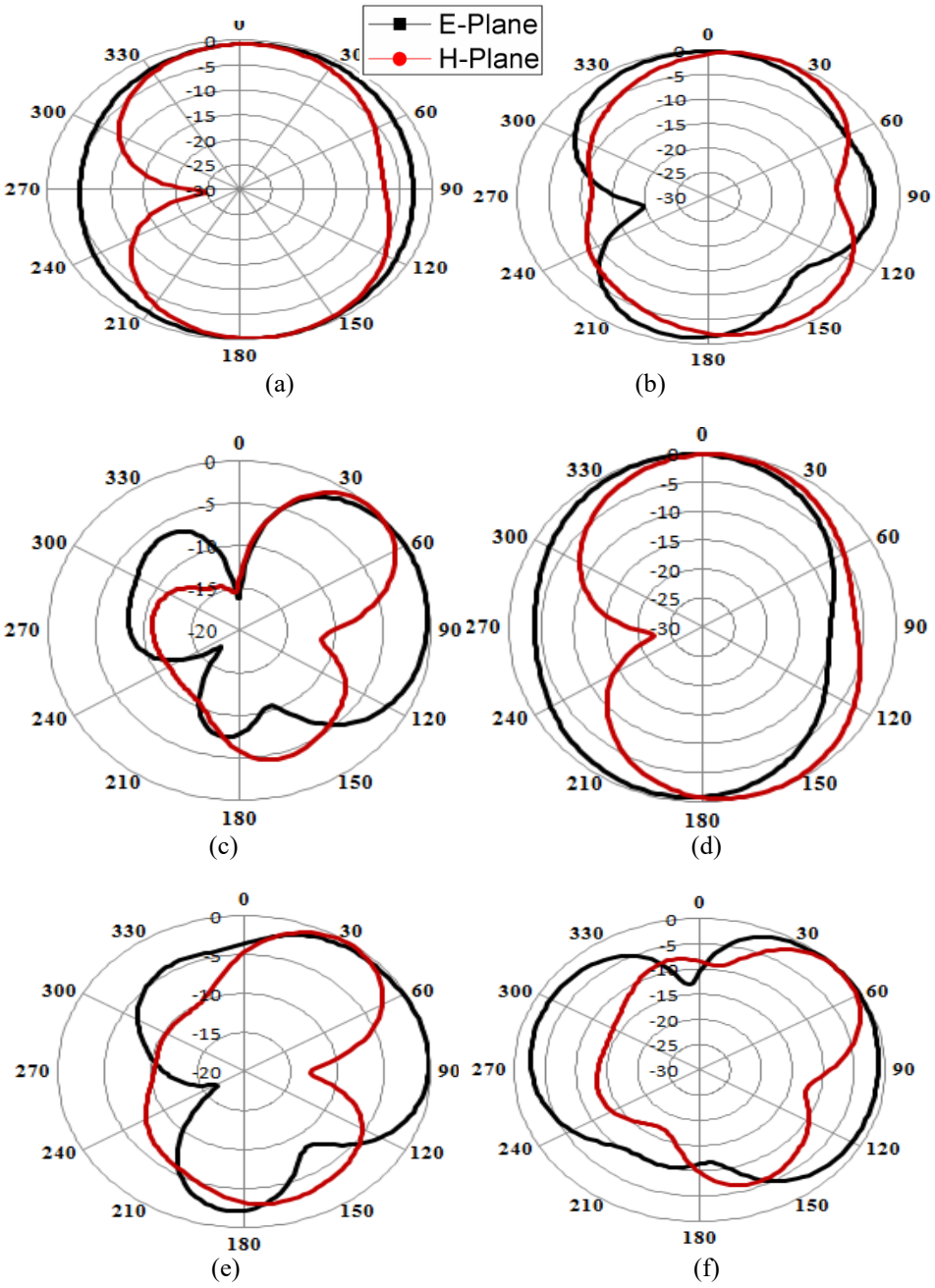

Figure-11. Patterns of the proposed annular ring crescent antenna.
(a) 3.1 GHz (b) 9.3 GHz.

Figure-12. Measurement of VSWR and Fabrication setup of the proposed antenna.

In-depth studies are carried out on the suggested UWB antenna's performance. The slot lengths (L1 and L2) are systematically changed and tuned to achieve a notched band over WiMAX and WLAN. The traditional UWB circular patch antenna was first simulated, and over the whole design frequency range, a VSWR of less than 2 and values of S11 less than -10 dB were found. Figure-8 compares the last iteration's simulated and measured VSWR performance. Figure-9 depicts the impedance's imaginary and real parts. Figure-10 shows the antenna's current fields at 3.1 GHz and 9.3 GHz. The figure also depicts electric fields and surface currents.

The patterns are also observed in Figure-11. The E-plane in Figure-11(a) resembles an omnidirectional plane. At the same time, the second one produces bidirectional patterns. The E- and H-plane patterns are visible in the semi-omnidirectional, according to Figure-11(b). The device's input impedance matching is also noted. The obtained VSWR findings are above 2, as observed from the outcome, and the antenna has demonstrated a notched band across WLAN. Figure-12 clarifies the fabrication setup of the proposed antenna. In addition, frequency shift away from the intended notched band is caused by increasing the split ring resonator's circular radius. The performance of the surface current of the antenna in different frequency variations is also given in Figure-13.

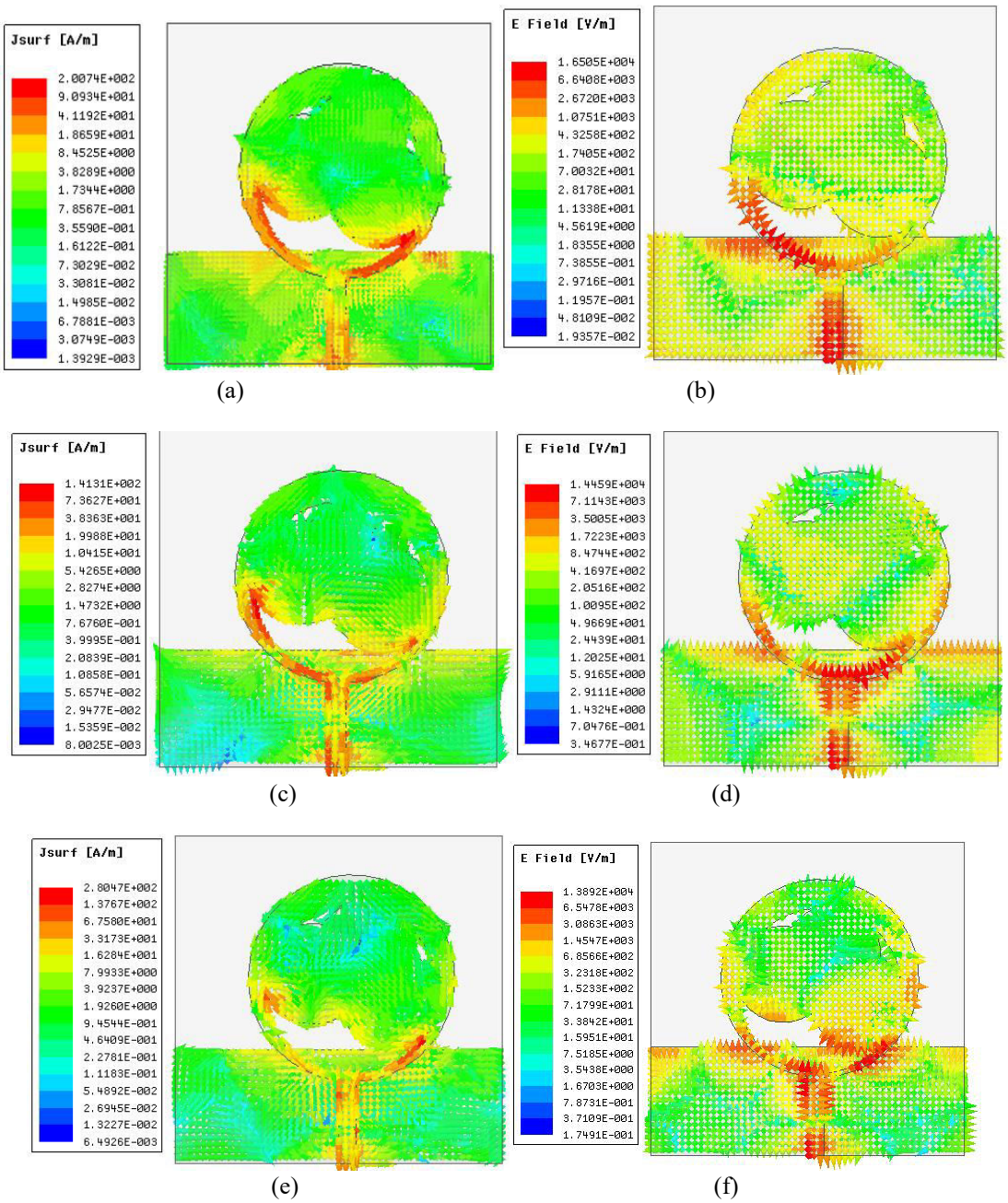

Figure-13. Surface currents at (a, b) 4.8 GHz Surface currents and E-fields (c, d) 7.29 GHz Surface currents and E-fields (e, f) 9.3 GHz Surface currents and E-fields.

Table-3. Comparison of the features of the proposed antenna.

Proposed antenna	Frequency (GHz)	Return loss (dB)	Bandwidth (GHz)
Simulated	4.6 7.29 9.36	-19.9 -26 -22.1	7.3
Measured	4.8 6.9 9.31	-40.01 -44.6 -16.4	7.1

The device's existing simulated areas are also provided at two operating bands. The experimental findings show the fewest discrepancies. The antenna's bandwidth is shown in Table-3, although the simulation does not account for mismatch losses because manufacturing defects are minor. The second band obtains good bandwidth when compared to the two bandwidth values. The intriguing aspect of this work is greater bandwidth. The antenna delivers 500 MHz bandwidth when it operates at 3.1 GHz. The measured bandwidth is 7.1 GHz from 3.3 to 10.96 GHz frequency. The antenna acquires a greater bandwidth when operating at 10.96 GHz frequency. The circular patches make it possible to get good gain and a wider impedance. The bandwidth obtained by the circular rings, which have suitable impedance, is used in various applications.

Table-4. Comparison of the proposed work with the existing literature survey.

Ref. No	Size (mm)	Freq (GHz)	Gain (dB)
[31]	50 × 30 × 1.6	1.81, 3.7, 5.9, 8.94, 12.7,	6.5 dBi
[32]	45×50×1.6	3.32-3.65 4.67-5.15	5.12 5.02
[33]	70×70×0.8	1.66-2.71	9.5
[34]	48×35×0.8	1.6-3	6.8
This work	38×38×1.6	4.8,6.9,9.31	6.51

5. CONCLUSIONS

In this article, a circular patch antenna is introduced for UWB applications. The reported antenna is compact, measuring 38 mm x 38 mm. The proposed antenna consists of a split ring resonator slot and, three smaller circles are united together finally mounted on the split ring resonator. The proposed antenna is fabricated with FR4 material with a 1.60 mm depth and a 4.4 relative permittivity. The reported antenna is measured following the manufacturing of the prototype design using both HFSS simulations. The findings demonstrate that when combined with VSWR 2, the reflection coefficient covers the band ranging from 3.3 to 10.96 GHz. The reported antenna has significant bandwidth and a maximum gain of 6.5 dBi. The outcome demonstrates the consistent radiation pattern across the whole UWB frequency range.

REFERENCES

[1] I. Falade O. P., Rehman M. U., Gao Y., *et al*. 2012. Single feed stacked patch circular polarized antenna for triple band GPS receivers. IEEE Trans. Antennas Propag. 60(10): 4479-4484.

[2] Jhamb K., Li L., Rambabu K. 2011. Novel-integrated patch antennas with multi-band characteristics. IET Microw. Antennas Propag. 5(12): 1393-1398.

[3] Bakariya P. S., Dwari S., Sarkar M., *et al*. 2015. Proximity-coupled microstrip antenna for Bluetooth, WiMAX, and WLAN applications. IEEE Antennas Wirel. Propag. Lett. 14, pp. 755-758.

[4] Bayatmaku N., Lotfi P., Azarmanesh M., *et al*. 2011. Design of simple multi-band patch antenna for mobile communication applications using new E-shape fractal. IEEE Antennas Wirel. Propag. Lett. 10, pp. 873-875.

[5] Singh A. K., Gangwar R. K., Kanaujia B. K. 2015. Orthogonal slot-loaded coaxially stacked annular ring antenna with circular patch for multi-band applications. J. Electromagn. Waves Appl. 29(12): 1630-1643.

[6] Singh V., Mishra B., Tripathi P. N., *et al*. 2016. A compact quad-band microstrip antenna for S and C-band applications. Microw. Opt. Technol. Lett. 58(6): 1365-1369.

[7] Parkash D., Khanna R. 2014. Multiband antenna structure for heterogeneous wireless communication systems using the DGS technique. Int. J. Microw. Wirel. Technol. 6(5): 521-526.

[8] Li M., Luk K. M. 2013. A low-profile wideband planar antenna. IEEE Trans Antennas Propag. 61: 4411-4418.

[9] Zhu J., Eleftheriades G. V. 2009. A compact transmission-line metamaterial antenna with extended bandwidth. IEEE Antennas Wirel Propag Lett. 8: 295-298.

[10] Lai C. P., Chiu S. C., Li H. J., Chen S. Y. 2011. Zeroth-order resonator antennas using inductor-loaded and capacitor-loaded CPWs. IEEE Trans Antennas Propag. 59: 3448-3453.

[11] Gupta A., Chaudhary R. K. 2015. A compact CPW fed wideband metamaterial antenna with EBG loading. Microw Opt Technol Lett. 57: 2632-2636.

[12] Sharma S. K., Gupta A., Chaudhary R. K. 2015. Epsilon negative CPW-fed zerothorder resonating antenna with backed ground plane for extended bandwidth and miniaturization. IEEE Trans Antennas Propag. 63: 5197-5203.

[13] Sonak R., Ameen M., Chaudhary R. K. 2018. Compact antenna based on SRR using radial stub as a virtual ground for wireless applications. 3rd International Conference on Microwave and Photonics (ICMAP). 1-2.

[14] Si L. M., Zhu W., Sun H. J. 213. A compact planar and CPW-fed metamaterial-inspired dual-band antenna. IEEE Antennas Wirel Propag Lett. 12: 305-308.

[15] Gupta A., Chaudhary R. K. 2106. A compact dual-band short ended metamaterial antenna with extended bandwidth. Int J RF Microwave Comput-Aided Engg. 26: 435-441.

[16] Sharma S. K., Chaudhary R. K. 2015. A compact zeroth-order resonating wideband antenna with dual-band characteristics. IEEE Antennas Wirel Propag Lett. 14: 1670-1672.

[17] Zarrabi F. B., Ahmadian R., Rahimi M., Mansouri Z. 2015. Dual band antenna designing with composite right/left handed. Microw Opt Technol Lett. 57: 774-779.

[18] C. A. Balanis. 1982. Antenna Theory. 2nd Ed, John Wiley & Sons, Inc., New York.

[19] D. Sinchez-Hemindez and I. Robertson. 1995. Analysis and design of a dual band circularly polarized microstrip patch antenna. IEEE Transactions on Antennas and Propagation. 43: 201-205.

[20] H. T. Nguyen, S. Noghanian, and L. Shafai. 2005. Microstrip patch miniaturization by Slot loading. In Proc. IEEE Inst. Symp. Antennas Propagation. pp. 215-218.

[21] J.-W. Wu, H.-M. Hsiao, J.-H. Lu and S.-H. Chang. 2004. Dualbroad band design of rectangular Slot antenna for 2.4 GHz and 5 GHz Wireless Communication. Electronic letter. 40: 1461-1463.

[22] K. F. Lee, K. M. Luk, K. M. Mak and S. L. S. Yang. 2011. On the use of U-slot design of dual and triple band patch antennas. IEEE Antennas Propagation Mag. 53(3): 60-74.

[23] U. Chakraborty, A. Kundu, S. K. Chawdhury and A. K. Bhattacharjee. 2014. Compact dual-band microstrip antenna for IEEE802.11a WLAN application. IEEE Antenna wireless propagation letter. 13: 407-410.

[24] T. M. Au and K. M. LuK. 1991. Effect of parasitic element on the characterstic microstrip antenna. IEEE Transaction on Antenna and Propagation. 39(8): 1247-1251.

[25] Ali Tanweer, Mohammad Saadh Aw, and Rajashekhar C. Biradar. 2018. A Compact Bandwidth Enhanced Antenna Loaded with SRR For WLAN/WiMAX/Satellite Applications. Advanced Electromagnetics. 7(4): 78-84.

[26] Omaima Benkhadda, Mohamed Saih, Kebir Chaji, Sarosh Ahmad and amp, Abdelati Reha. 2023. Miniaturized tri-band fractal antenna design for LTE, WLAN, WiMAX, and C-band applications. International Journal of Electronics, DOI: 10.1080/00207217.2023.2248658.

[27] S. Ahmad *et al*. and quot. 2021. A Metasurface-Based Single-Layered Compact AMC-Backed Dual-Band Antenna for Off-Body IoT Devices, & quot; in IEEE Access, 9: 159598-159615, doi: 10.1109/ACCESS.2021.3130425.

[28] Sellak L., Khabba A., Chabaa S., *et al*. 2023. ANFIS-Based Dual Band Circular MIMO Antenna Design with Pretty- Small Size and Large Bandwidth for 5 G Millimeter-Wave Applications at 28/38 GHz. J Infrared Milli Terahz Waves 44, 551-601. https://doi.org/10.1007/s10762-023-00924-3.

[29] F. Ez-Zaki *et al*. & quot. 2023. Double Negative (DNG) Metamaterial-Based Koch Fractal MIMO Antenna Design for Sub-6-GHz V2X Communication, & quot; in IEEE Access, 11: 77620-77635, doi: 10.1109/ACCESS.2023.3296599.

[30] S. Nej, A. Ghosh, S. Ahmad, J. Kumar, A. Ghaffar and M. I. Hussein. 2022. Design and Characterization of 10-Elements MIMO Antenna with Improved Isolation and Radiation Characteristics for mm-Wave 5G Applications. In IEEE Access, 10: 125086-125101, doi: 10.1109/ACCESS.2022.3225446.

[31] Bag Biplab, *et al*. and quot; 2020. A wide multi-band monopole antenna for GSM/WiMAX/WLAN/X-band/Ku-band applications. And quot; Wireless Personal Communications 111: 411-427.

[32] Li Y., Zhao Z., Tang Z. and amp Yin, Y. 2019. A low-profile, dual-band filtering antenna with high selectivity for 5G sub-6 GHz applications. Microwave and Optical Technology Letters. 61(10): 2282-2287.

[33] Yang Y., Zhang J., Lan H. and amp Liu M. 2019. A low-profile wideband dual-polarization patch antenna with an antisymmetric feeding network. International Journal of RF and Microwave Computer-Aided Engineering. 29(10): e21877.

[34] Chopra R. and amp Kumar G. 2020. Compact, broadband, and high gain directional end-fire antenna. Microwave and Optical Technology Letters, 62(7): 2546-2553.